Reducing the Molecule-Substrate Coupling in C_{60}-Based Nanostructures by Molecular Interactions

K. J. Franke,[1,*] G. Schulze,[1] N. Henningsen,[1] I. Fernández-Torrente,[1] J. I. Pascual,[1] S. Zarwell,[2] K. Rück-Braun,[2] M. Cobian,[3] and N. Lorente[3,4]

[1]*Institut für Experimentalphysik, Freie Universität Berlin, Arnimallee 14, 14195 Berlin, Germany*
[2]*Institut für Chemie, Technische Universität Berlin, Strasse des 17. Juni 135, 10623 Berlin, Germany*
[3]*Institut de Ciència de Materials de Barcelona (CSIC), Campus de la UAB, 08193 Bellaterra, Spain*
[4]*Centre d'Investigació en Nanociència i Nanotecnologia (CSIC-ICN), Campus de la UAB, 08193 Bellaterra, Spain*

(Received 3 August 2007; published 24 January 2008)

Codeposition of C_{60} and the three-dimensional molecular hydrocarbon 1,3,5,7-tetraphenyladamantane (TPA) on Au(111) leads to the spontaneous formation of molecular nanostructures in which each fullerene is locked into a specific orientation by three surrounding TPA. Scanning tunneling spectroscopy shows that the electronic coupling of C_{60} with the surface is significantly reduced in these nanostructures, enhancing the free-molecule properties. As evidenced by density functional theory simulations, the nanostructures are stabilized by 18 local electrostatic forces between C_{60} and TPA, resulting in a lifting of the C_{60} cage from the surface.

DOI: 10.1103/PhysRevLett.100.036807 PACS numbers: 73.22.−f, 68.37.Ef, 73.61.Wp, 73.63.−b

The use of organic molecular thin films on an inorganic surface [1,2] offers the perspective of tuning their electronic functionality by redesigning the basic molecular components. At the interface with a metal, the molecular levels are pinned due to hybridization and charge transfer processes [3], resulting in a substantial broadening of the molecular resonances. The performance of molecular interfaces in, for example, electronic devices depends on the facility of charge injection, but also on fundamental parameters regarding carrier mobility and lifetime. Polaronic charge transport and luminescence [4] are strongly improved by the localization of electronic states in the molecular layer. It is hence desirable to design strategies that permit us to modify the degree of electronic coupling between molecular entities with states of the metallic support.

A recent approach to weaken the electronic interaction between a molecular layer and an inorganic interface is to use dielectric spacers, thin enough to allow charge injection. Ultrathin films of oxides [5–9], ionic salts [4,10,11], nitride [12], or alkanethiol layers [13,14] have been used to successfully decrease the electronic overlapping between an atom or a molecule and a metal surface. The results of such spacers are, for example, the sharpening of molecular resonances [13,14], giving rise to strong nonlinearities in charge transport, an increase in their electronic lifetime and coupling with vibrations in the molecule [9], improving photoluminescence efficiency [4,7], or the decrease of exchange interactions of an atom with the metal, hence allowing the control of magnetization at the atomic level [12].

Here, we report on an alternative approach to weaken the electronic coupling between a molecule and a metallic surface, based on lateral electrostatic interactions of two organic molecules. These interactions lift one of the species from the surface and at the same time allow the molecule to recover its gas phase shape. We show that C_{60} with 1,3,5,7-tetraphenyladamantane (TPA) spontaneously forms nanostructures on Au(111), where one C_{60} molecule is surrounded by three TPA. These nanostructures are stabilized by multiple electrostatic intermolecular bonds between hydrogen atoms and fullerene π states, as resolved by numerical simulations of the bonding induced charge density. Unexpectedly, these bonds are very local and, instead of distorting the cage structure, cause the C_{60} cage to be reoriented and lifted from the surface, restoring its free-molecule structure and its electronic integrity, as evidenced by scanning tunneling spectroscopy (STS). These results foretell a new approach for tuning molecule-surface coupling by the proper functionalization of the interacting molecules, which in this case is proven to be mediated by noncovalent interactions to a conjugated cage.

We chose TPA as a hydrocarbon to interact with C_{60} [Figs. 1(a) and 1(c)], because its concave carbon skeleton makes this molecule a good candidate to form an inclusion complex with the curved conjugated carbon cage of C_{60}. The large difference in gap between TPA and C_{60} [20] implies a very small intermolecular hybridization of the frontier orbitals leading to a reduction of electron transport from C_{60} into the metal substrate via TPA orbitals.

TPA was deposited on the Au(111) surface by sublimation under ultrahigh vacuum conditions. The Au(111) surface, previously cleaned using standard sputter-annealing methods, was kept at room temperature during the adsorption of about 0.5 monolayers of TPA and subsequent deposition of C_{60}. Scanning tunneling microscopy (STM) and STS measurements were then carried out at 4.8 K in custom-made equipment.

Figures 1(a) and 1(b) show typical STM images. The most characteristic features are triangular shaped arrangements attributed to TPA/C_{60} mixed nanostructures. The close-up view in Fig. 1(c) resolves that the smallest nano-

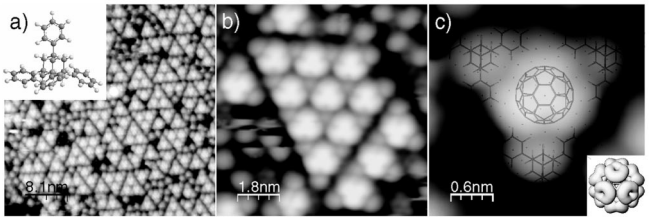

FIG. 1. (a) Large scale STM image [15] of empty states ($I = 25$ pA, $V_S = 600$ mV, bias is referred to sample bias) of TPA and C_{60} on Au(111) (inset: model of TPA). (b) Self-assembled complex of TPA/C_{60} revealing that each fullerene is in the same local arrangement. (c) STM image of the smallest TPA/C_{60} complex ($I = 25$ pA, $V_S = 870$ mV). The small protrusions correspond to TPA, while the large ones with threefold symmetry represent C_{60}. The latter is always oriented with a C3 axis perpendicular to the surface [compare to the lowest unoccupied molecular orbital (LUMO) isosurface in the inset [16]]. The molecular structure as minimized by force-field calculations is superimposed [17].

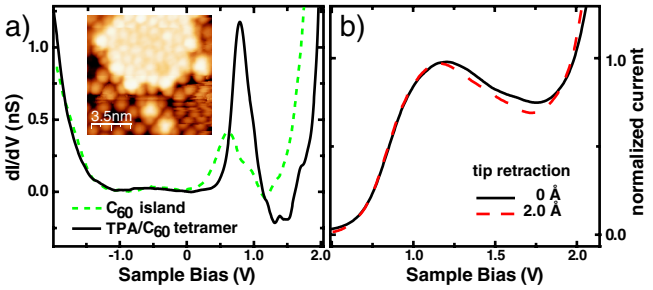

FIG. 2 (color online). (a) dI/dV curves ($V_{ac} = 7$ mV rms, $V_S = 2.3$ V, $I_t = 1.1$ nA) recorded on a TPA/C_{60} tetramer and on a pure C_{60} island (see the inset). In the same image the C_{60} orbitals are clearly visible in the tetramers while they are more blurred in the island. (b) I-V curves acquired with different widths of the tunnel barrier. After opening the feedback loop ($V_S = 2.3$ V, $I_t = 1$ nA), the tip has been retracted by 0 Å and 2 Å, respectively. Each curve is normalized to the local current maximum of the LUMO. Negative differential resistance increases for larger tip-sample distances.

structure consists of a single fullerene at the center of a triangle, whose vertices are formed by three TPA molecules, seen as three lower protrusions. These tetramers are the basic building block of periodically extended structures as those shown in Fig. 1(b). Interestingly, in the TPA/C_{60} complexes, C_{60} is always found in the same orientation as revealed by the threefold shape of the intramolecular structure [Figs. 1(b) and 1(c)]. This specific internal structure of the fullerene corresponds to the characteristic shape of the LUMO when a C3 axis is oriented perpendicular to the surface [16]. It should be noted that in pure C_{60} islands on Au(111), found occasionally in this preparation, the molecular cage exhibits a large variety of orientations [21,22]. Hence, from the unique orientation in the nanostructures a local interaction between C_{60} and TPA can be inferred.

An indication of the C_{60} molecular orbitals being less perturbed by the surface in the tetramers is given by the fact that their intermolecular structure is more clearly resolved than in pure C_{60} islands with the same tip conditions [11]. In order to resolve the electronic configuration of the TPA/C_{60} complex we recorded the current-voltage and differential conductance (dI/dV)—voltage characteristics. A typical dI/dV spectrum of TPA/C_{60} complexes is presented in Fig. 2(a) [23]. A gap of about 2.6 eV width is observed, limited by two nonlinear features associated with the energetic position of the LUMO and highest occupied molecular orbital (HOMO) derived resonances. The LUMO peak of C_{60} in the TPA/C_{60} nanostructure is significantly sharper (FWHM $\sim$ 290 meV) than in a pure C_{60} island (FWHM $\sim$ 400 meV). Additionally, the LUMO position of C_{60} in a tetramer is shifted by $\sim$200 meV to higher energies than for molecules in the pure island. An increase in gap width is expected for a more weakly coupled molecule, since the screening of the substrate is reduced leading to a larger Coulomb repulsion of the tunneling electron [24].

A further intriguing feature in the spectra of C_{60} in the TPA/C_{60} complex is a regime of negative differential resistance (NDR) in the high-energy part of the LUMO, which is neither found on pure C_{60} islands nor on TPA regions. NDR is a fingerprint in tunneling dI/dV spectra of localized states weakly coupled with the supporting electrode [11,25]. The origin of this effect lies in the rapid energy dependence of the vacuum transmittivity, but requires for its observation the presence of sharp resonances, as has been described by Grobis *et al.* [25]. A characteristic of this effect is that it becomes more pronounced with the tip-sample distance, as is found in our case [Fig. 2(b)] [26]. Thus, NDR is compatible with the presence of a sharper LUMO resonance in the TPA/C_{60} complex. In addition to the observation of a larger gap width and a sharper intramolecular structure, this reflects a significant reduction in the electronic coupling strength of the fullerenes with the metallic substrate.

In order to understand the origin for this weaker electronic coupling and the role of molecular interactions between C_{60} and TPA we have performed density functional theory calculations with the VASP code [27]. According to the experimental results [Fig. 1(b)] and in agreement with force-field simulations [Fig. 1(c)] [17], the periodically extended structure of the TPA/C_{60} complexes corresponds to a $2\sqrt{7} \times 2\sqrt{7}$ $R19°$ unit cell, taken as a starting point for the density-functional theory (DFT) simulations in order to reduce the computational effort. The Au(111) substrate was modeled by 4 fcc layers, leading to a 238-atom unit cell. Because of the periodic boundary conditions in the z direction we keep a minimum separation of 11 Å between the topmost molecular atom and the bottom layer of the next gold slab. We found that the local density approximation (LDA) gives an Au lattice parameter, which is 0.01 Å shorter than the experimental one, permitting us to remain very close to the experimental

geometry [28]. In the minimized structure, C_{60} lies on top of a gold atom and is held by the three surrounding TPAs, which sit on the surface with three of their phenyl moieties in an almost flat configuration, as depicted in Fig. 3(a). Consistent with the experimental data, C_{60} in a TPA/C_{60} complex shows the same azimuthal orientation with a hexagon facing upward. A corresponding simulated STM image at positive sample bias according to Tersoff-Hamann theory shows the pronounced threefold structure of the C_{60}'s LUMO and the smaller protrusions due to TPA in good agreement with the experimental data [Figs. 3(b) and 3(c)]. The closest distance between TPA and C_{60} is 2.8 Å. The distance of C_{60} from the surface plane is 2.8 Å. The molecular cage is only slightly distorted from its free-molecule shape (≤ 1 pm). If the TPAs are removed, the C_{60} gets closer to the surface by 0.58 Å and the cage is deformed by ≈ 5 pm.

In order to resolve whether the lifting of C_{60} is the main reason for the reduced coupling with the surface as observed in the experiment, we have calculated the TPA/C_{60} electronic structure and compared it with that of a C_{60} island with a $2\sqrt{3} \times 2\sqrt{3}$ $R30°$ structure [21], as in the experiments shown in Fig. 2(a). The density of states projected onto chosen molecular orbitals of the corresponding free molecule (PDOS) yields the weight of the particular orbital in the total electronic structure of the whole molecule-surface system. It therefore permits us to resolve the perturbation and alignment of the molecular orbitals upon adsorption [29]. In Figs. 3(d) and 3(e) we compare the PDOS on C_{60} molecular orbitals in the pure island case with the PDOS in the TPA/C_{60} nanostructures.

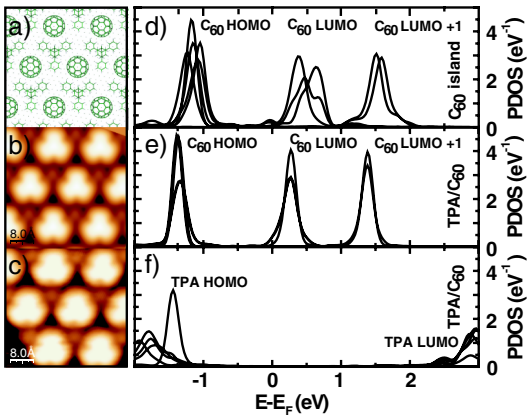

FIG. 3 (color online). (a) $2\sqrt{7} \times 2\sqrt{7}$ $R19°$ model structure of the molecular arrangements as minimized by DFT on Au(111). (b) Corresponding simulated STM image at $V_S = 500$ mV within the Tersoff-Hamann theory. (c) Experimental constant current STM image at $I = 25$ pA, $V_S = 870$ mV. (d) Projected density of states (PDOS) on C_{60} in a monolayer corresponding to the $2\sqrt{3} \times 2\sqrt{3}$ $R30°$ structure. The HOMO and LUMO degeneracy is broken due to intermolecular and molecule-substrate interactions. (e) PDOS on C_{60} in the TPA/C_{60} nanostructure. (f) PDOS on TPA in the TPA/C_{60} nanostructure of (e). For numerical reasons a Gaussian broadening of 0.1 eV was used.

In the former the molecular orbitals are significantly perturbed by the substrate. Because of the interaction with the surface the degeneracy of the fivefold HOMO and threefold LUMO is removed. This symmetry breaking leads to a substantially broadened LUMO peak, in agreement with the experimentally derived LUMO resonance of about 400-meV width. In contrast, C_{60} in the TPA/C_{60} nanostructures [Fig. 3(e)] preserves the degeneracy of the HOMO and the LUMO, in agreement with the undistorted cage structure. Therefore, the corresponding peaks appear with much thinner overall line shapes, in accordance with the smaller LUMO width in the tunneling spectra.

It is surprising that the C_{60} cage structure is not perturbed, although the interaction with TPA is sufficiently strong to lift and orient the fullerene. Moreover, the C_{60} is seeing insulating TPA molecules as can be concluded from the PDOS on TPA and their localization in space. The TPA's HOMO and LUMO at -1.5 eV and 2.5 eV, respectively, are formed by π states with their main weight in the phenyl rings [Fig. 3(f)] [30]. Therefore, both the TPA's HOMO and LUMO are spatially lying far away from the C_{60} cage. States in the adamantane core have a σ character and are far outside of this energy window. Thus, there is no hybridization between the C_{60}'s HOMO and LUMO resonances with TPA states. The nature of the interaction between TPA and C_{60}, which leads to the lifting from the surface and locking of the fullerene's orientation, is hence of noncovalent origin.

An insight in the bonding can be obtained by analyzing maps of the induced charge density, which reveal the perturbation of the electronic structure of the whole system by the inclusion of the considered molecule [31]. The interaction of C_{60} with TPA/Au(111) is given by the change in charge density induced by the presence of C_{60} in the TPA/C_{60}/Au(111) relaxed structure (Fig. 4). An

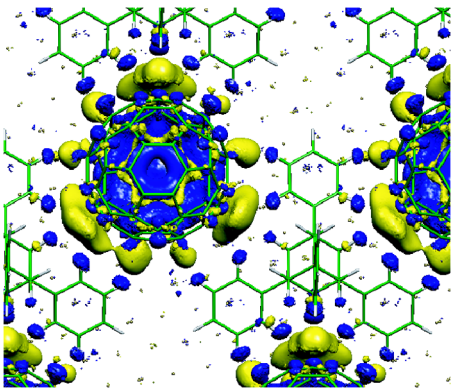

FIG. 4 (color online). Induced charge density with an isosurface contour at 0.0002 $e/Å^3$ due to the interaction of C_{60} with the TPA/Au(111) system (darker and lighter colors represent electron depletion and electron excess, respectively). An excess of electron density is found near the double bonds of C_{60}, while an electron depletion is localized on nearby H atoms. This points to a local electrostatic interaction between the molecules which dictates the orientation and lifting of C_{60} from the surface.

increase in electron density is found localized around the double bonds of the fullerene cage. Opposite to these there are 18 electron depleted regions at the hydrogen atoms of the surrounding TPA. The strongest correspond to the (positively charged) sp^3-hybridized H atoms of the adamantane cage pointing toward the closest (electron rich) double bonds of C_{60}. This induced density then reveals the presence of charges of opposite signs, hence giving rise to an attractive electrostatic interaction between the molecules. The overall C_{60}–TPA interaction energy amounts to ~0.6 eV leading to an average of 35 meV for each of the 18 C-H pairs. The chemisorption energy of C_{60} in the TPA/C_{60} complex is 1.10 eV. Therefore, the direct C_{60}–surface interaction is estimated as ~0.5 eV, lower than the 0.86 eV chemisorption energy of C_{60} in the $2\sqrt{3} \times 2\sqrt{3}$ $R30°$ structure [32]. Comparison of the chemisorption energies of C_{60} in the tetramer and in the homomolecular islands thus supports the reduced interaction of the fullerene with the surface and further reflects the more stable nature of the TPA/C_{60} nanostructures.

Hence, the attractive interaction between opposite charges induced on C_{60} and TPA is similar to the electrostatic character of CH-π bonds in fullerene chemistry [33]. The number of these bonds is maximized when the fullerene cage is in the C3 orientation. This is the driving force for the orientation and lifting of C_{60} from the surface. The effect of the TPA molecules is thus twofold: they reduce the direct C_{60}–substrate interaction, and they stabilize the C_{60} in the nanostructures.

In conclusion, we have presented a new approach for reducing the direct coupling of organic molecules to a metallic substrate. Instead of the inclusion of spacer layers, we have shown that lateral molecular interactions, such as the electrostatic attraction of electron rich and depleted areas of C_{60} and TPA, are capable of partially overcoming the direct C_{60}–surface bonding. Functionalizing the molecules opens the possibility of tuning the molecule-surface interactions. It will therefore permit us to create nanostructures with tailored electronic properties on the molecular scale.

This research was supported by the DFG through Nos. Sfb 658 and SPP 1243. N. L. and M. C. acknowledge support from Spanish MEC (No. FIS2006-12117-C04-01) and computer time from CESCA. I. F.-T. acknowledges support from the Generalitat de Catalunya.

*Corresponding author.
franke@physik.fu-berlin.de

[1] H. Park *et al.*, Nature (London) **407**, 57 (2000).
[2] N. Takahashi *et al.*, Appl. Phys. Lett. **90**, 083503 (2007).
[3] N. Koch *et al.*, Phys. Rev. Lett. **95**, 237601 (2005).
[4] E. Cavar *et al.*, Phys. Rev. Lett. **95**, 196102 (2005).
[5] X. H. Qiu, G. V. Nazin, and W. Ho, Science **299**, 542 (2003).
[6] N. Nilius, T. M. Wallis, and W. Ho, Phys. Rev. Lett. **90**, 046808 (2003).
[7] X. H. Qiu, G. V. Nazin, and W. Ho, Phys. Rev. Lett. **92**, 206102 (2004).
[8] A. J. Heinrich *et al.*, Science **306**, 466 (2004).
[9] G. V. Nazin, S. W. Wu, and W. Ho, Proc. Natl. Acad. Sci. U.S.A. **102**, 8832 (2005).
[10] J. Repp *et al.*, Phys. Rev. Lett. **95**, 225503 (2005).
[11] J. Repp *et al.*, Phys. Rev. Lett. **94**, 026803 (2005).
[12] C. F. Hirjibehedin, C. P. Lutz, and A. J. Heinrich, Science **312**, 1021 (2006).
[13] J. Zhao *et al.*, Phys. Rev. Lett. **95**, 045502 (2005).
[14] B. Li *et al.*, J. Chem. Phys. **124**, 064709 (2006).
[15] I. Horcas *et al.*, Rev. Sci. Instrum. **78**, 013705 (2007).
[16] J. I. Pascual *et al.*, J. Chem. Phys. **117**, 9531 (2002).
[17] We have carried out molecular mechanics simulations as implemented in the TINKER package (MM3 force field) [18,19]. Simulated annealing (30 000 steps for cooling from 250 to 0 K) gives the minimum energy configuration as illustrated in Fig. 1(c).
[18] J. W. Ponder©, http://dasher.wustl.edu/tinker.
[19] N. L. Allinger, Y. H. Yuh, and J. H. Lii, J. Am. Chem. Soc. **111**, 8551 (1989).
[20] The HOMO-LUMO gap of TPA is 3 times larger than in C_{60} as obtained by our DFT calculations.
[21] C. Rogero *et al.*, J. Chem. Phys. **116**, 832 (2002).
[22] X. H. Lu *et al.*, Phys. Rev. B **70**, 115418 (2004).
[23] The electronic fingerprint of a C_{60} in a single tetramer is found to be the same as on the periodically extended structures.
[24] R. Hesper, L. H. Tjeng, and G. A. Sawatzky, Europhys. Lett. **40**, 177 (1997).
[25] M. Grobis *et al.*, Appl. Phys. Lett. **86**, 204102 (2005).
[26] The observation of this tip-sample dependence also excludes other possible mechanisms leading to NDR, such as instabilities of the molecule in the tunneling junction as these would be more pronounced for smaller tip-molecule distances.
[27] G. Kresse and J. Fürthmuller, Comput. Mater. Sci. **6**, 15 (1996).
[28] We have used the relativistic PAW pseudopotential included in VASP for LDA. This is crucial to obtain simulation geometries that agree with the experimental ones. The two topmost gold layers and molecules were relaxed to forces smaller than 0.03 eV/Å. A $3 \times 3 \times 1$ k-point set was used due to the extended nature of the interactions as mediated by the substrate. The plane wave basis set was expanded with a 400-eV cutoff. Our calculations using the generalized gradient approximation (GGA) lead to the same qualitative result.
[29] H. Lesnard, M.-L. Bocquet, and N. Lorente, J. Am. Chem. Soc. **129**, 4298 (2007).
[30] The sharpest peak corresponds to the phenyl ring pointing upright. The states in the phenyl rings close to the surface are broader because they are hybridized with the d states of Au(111).
[31] G. Witte *et al.*, Appl. Phys. Lett. **87**, 263502 (2005).
[32] L.-L. Wang and H.-P. Cheng, Phys. Rev. B **69**, 165417 (2004).
[33] H. Suezawa *et al.*, CrystEngComm. **5**, 514 (2003).